Ecotoxicology and Environmental Safety 262 (2023) 115113

Contents lists available at ScienceDirect

Ecotoxicology and Environmental Safety

journal homepage: www.elsevier.com/locate/ecoenv

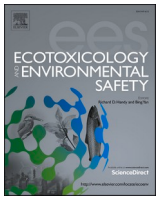

Migration of polycyclic aromatic hydrocarbons from a polymer surrogate through the *stratum corneum* layer of the skin

Konstantin Simon [a,b,*], Lidia Schneider [a], Gila Oberender [a,c], Ralph Pirow [a], Christoph Hutzler [a], Andreas Luch [a,b], Alexander Roloff [a,**]

[a] German Federal Institute for Risk Assessment (BfR), Department of Chemical and Product Safety, Max-Dohrn-Str. 8–10, 10589 Berlin, Germany
[b] Department of Biology, Chemistry, Pharmacy, Institute of Pharmacy, Freie Universität Berlin, Königin-Luise-Str. 2–4, 14195 Berlin, Germany
[c] Berliner Hochschule für Technik (BHT), Luxemburger Str. 10, 13353 Berlin, Germany

ARTICLE INFO

Editor: Dr Hyo-Bang Moon

Keywords:
stratum corneum
skin migration
polycyclic aromatic hydrocabons (PAH)
partition
diffusion

ABSTRACT

In this study, we determined partition ($K_{sc/m}$) and diffusion (D_{sc}) coefficients of five different polycyclic aromatic hydrocarbons (PAH) migrating from squalane into and through the *stratum corneum* (s.c.) layer of the skin. Carcinogenic PAH have previously been detected in numerous polymer-based consumer products, especially those dyed with carbon black. Upon dermal contact with these products, PAH may penetrate into and through the viable layers of the skin by passing the s.c. and thus may become bioavailable. Squalane, a frequent ingredient in cosmetics, has also been used as a polymer surrogate matrix in previous studies. $K_{sc/m}$ and D_{sc} are relevant parameters for risk assessment because they allow estimating the potential of a substance to become bioavailable upon dermal exposure. We developed an analytical method involving incubation of pigskin with naphthalene, anthracene, pyrene, benzo[*a*]pyrene and dibenzo[*a,h*]pyrene in Franz diffusion cell assays under quasi-infinite dose conditions. PAH were subsequently quantified within individual s.c. layers by gas chromatography coupled to tandem mass spectrometry. The resulting PAH depth profiles in the s.c. were fitted to a solution of Fick's second law of diffusion, yielding $K_{sc/m}$ and D_{sc}. The decadic logarithm log$K_{sc/m}$ ranged from −0.43 to +0.69 and showed a trend to higher values for PAH with higher molecular masses. D_{sc}, on the other hand, was similar for the four higher molecular mass PAH but about 4.6-fold lower than for naphthalene. Moreover, our data suggests that the s.c./viable epidermis boundary layer represents the most relevant barrier for the skin penetration of higher molecular mass PAH. Finally, we empirically derived a mathematical description of the concentration depth profiles that better fits our data. We correlated the resulting parameters to substance specific constants such as the logarithmic octanol-water partition coefficient log*P*, $K_{sc/m}$ and the removal rate at the s.c./viable epidermis boundary layer.

1. Introduction

Understanding the migration of polycyclic aromatic hydrocarbons (PAH) from consumer products through the skin is of key importance to support risk assessment of this ubiquitous class of contaminants. Exposure to PAH is linked to several relevant toxicological endpoints. For example, benzo[*a*]pyrene (B[*a*]P), one of the best studied PAH, can cause reproductive toxicity (Mackenzie and Murray Angevine, 1981), immune system suppression (Hardin et al., 1992), genotoxicity (Brinkmann et al., 2012) and cancer (Rota et al., 2014), among other adverse

Abbreviations: B[*a*]P, benzo[*a*]pyrene; c_m, concentration in medium; c_{sc}, concentration in *stratum corneum*; $c_{x,t}$, concentration at depth x and time t; c_{rel}, relative concentration; DB[*a,h*]P, dibenzo[*a,h*]pyrene; D_{sc}, diffusion coefficient in the *stratum corneum*; EFSA, European Food Safety Authority; FDC, Franz diffusion cell; GC-MS/MS, gas chromatography coupled to tandem mass spectrometry; H_{sc}, total thickness of *stratum corneum*; IARC, International Agency for Research on Cancer; $K_{sc/m}$, partition coefficient between stratum corneum and medium; log*P*, octanol-water partition coefficient; LOQ, limit of quantification; *M*, molecular mass; OECD, Organization for Economic Co-operation and Development; PAH, polycyclic aromatic hydrocarbons; s.c., *stratum corneum*; SCCS, Scientific Committee on Consumer Safety; SD, standard deviation; SI, supporting information; *t*, time; *x*, depth in *stratum corneum*; σ, residual standard deviation.

* Corresponding author at: German Federal Institute for Risk Assessment (BfR), Department of Chemical and Product Safety, Max-Dohrn-Str. 8–10, 10589 Berlin, Germany.
** Corresponding author.
E-mail addresses: Konstantin.Simon@bfr.bund.de (K. Simon), Alexander.Roloff@bfr.bund.de (A. Roloff).

https://doi.org/10.1016/j.ecoenv.2023.115113
Received 23 December 2022; Received in revised form 2 June 2023; Accepted 4 June 2023
Available online 12 June 2023

conditions (Collins et al., 1998). The International Agency for Research on Cancer (IARC) classifies B[*a*]P as a class 1 carcinogen, whereas many other PAH are considered to be possibly carcinogenic to humans (IARC, 2010; IARC, 2018). Multiple regulations have limited the amount of PAH in consumer products (Regulation (EC), 2006: Regulation (EU) 2013), although there is no safe exposure level for genotoxic carcinogens (BfR, 2019). Unfortunately, PAH are still detectable in certain commodities made of synthetic polymers, such as tools and toys (Alawi et al., 2018; Bartsch et al., 2017).

Upon dermal contact, these PAH have been shown to migrate through the *stratum corneum* (s.c.) into viable human skin layers, where they potentially become bioavailable (Bartsch et al., 2016). Most studies, however, investigated skin uptake from aqueous matrices (Luo et al., 2020; Roy et al., 2007; Sousa et al., 2022) or organic solvents such as acetone (Moody et al., 1995, 2011; Ng et al., 1991; Sartorelli et al., 1998), which are only of limited relevance for PAH exposure from consumer products. To the best of our knowledge, concentration profiles of these substances in the s.c. after dermal exposure have never been reported. Accordingly, we decided to study skin penetration of PAH from squalane. Squalane is a suitable surrogate for aliphatic polymers that has been used previously to investigate the stability of polymer additives (Barret et al., 2002; Soebianto et al., 1993; Bartsch, 2018; Beißmann et al., 2014). It is highly lipophilic (calculated octanol-water partition coefficient log$P$ = 15.6, Octanol-Water Partition Calculation, 2021) and resembles an extended and branched alkyl chain (Zafar and Chickos, 2019). Furthermore, it is frequently used as an ingredient in cosmetic articles, such as anti-aging creams, lotions and shampoos (Bergfeld et al., 2019; Kim and Karadeniz, 2012).

Upon first contact of a substance with the skin, partitioning occurs from the applied medium into the s.c., the outermost layer of the skin representing a crucial barrier for skin penetration (Sousa et al., 2022). This process is described by the partition coefficient $K_{sc/m}$, which is defined as the ratio of the concentration in the s.c. (c_{sc}) to the concentration in the medium (c_m; here: squalane) at chemical equilibrium. $K_{sc/m}$ is strongly dependent on the physicochemical properties of the medium in which the substance of interest is applied to the skin. Because the s.c. is comparatively lipophilic (Raykar et al., 1988), lipophilic substances are expected to have a higher partition coefficient, as was shown exemplarily by Rothe et al. (2017) for partitioning from aqueous media.

Partitioning of a substance into the upper most layer of the s.c. is followed by diffusion into deeper layers. This process is governed by Fick's (1855) laws of diffusion. The second law describes the concentration profile of a substance in a medium as a function of time:

$$\frac{\partial c_{x,t}}{\partial t} = -D_{sc}\frac{\partial^2 c_{x,t}}{\partial x^2}, \tag{1}$$

where $c_{x,t}$ is the concentration at depth x of the s.c. and time t, and D_{sc} is the diffusion coefficient in the s.c. D_{sc} is a measure of how fast a substance will move through the s.c. and reach the viable epidermis, where it will potentially become bioavailable.

In silico methods aiming to model partitioning and diffusion of substances through the skin crucially rely on input parameters — including $K_{sc/m}$ and D_{sc} — to predict skin permeation accurately. They can represent helpful alternatives to tedious *in vivo* studies on dermal exposure to toxic substances. However, *in vitro* skin permeation studies are needed to determine realistic input parameters. The present study contributes to this work with experimentally derived values for $K_{sc/m}$ and D_{sc} of highly lipophilic PAH (log$P$ = 3.4–7.4 (de Lima Ribeiro and Ferreira, 2003; US EPA, 2012) by employing Franz diffusion cell (FDC) assays (Franz, 1975). We investigated partitioning and diffusion of naphthalene, anthracene, pyrene, B[*a*]P and dibenzo[*a,h*]pyrene (DB[*a,h*]P) from squalane matrices into and through the s.c. of excised pigskin. These PAH feature molecules consisting of two to six condensed aromatic rings. To the best of our knowledge, this study is the first to measure these parameters for substances with a high carcinogenic potential applied in a matrix that is relevant for real-life exposure to polymer-based consumer products and cosmetics.

2. Methods

The following section summarizes the method applied in this work. A detailed description can be found in the supporting information (SI, section A.2 *Method*). The FDC assays were carried out with two different incubation times (1 h and 24 h) in replicates with $n = 4$ (24 h: naphthalene, pyrene, DB[*a,h*]P), $n = 8$ (24 h: B[*a*]P) and $n = 5$ (1 h: all PAH).

2.1. Principle of the Franz diffusion cell assay

The FDC assay (Franz, 1975) is a well-established method to investigate dermal absorption (Bartsch et al., 2018; Bronaugh et al., 1981, 1986, Bronaugh and Stewart, 1984, 1986; Ng et al., 2010) and was previously established for PAH at our institute (Bartsch et al., 2016). In this study, the receptor chamber at the bottom of the FDC (Fig. S1) contained bovine serum albumin (BSA; 50 mg·ml^{-1}) in Dulbecco's phosphate buffered saline (DPBS). BSA is known to increase the solubility of lipophilic substances in aqueous solutions, which is also its primary function in the bloodstream (Bronaugh and Stewart, 1984; Ellison et al., 2020, 2021; Gerstel et al., 2016). Furthermore, it can compensate for loss of protein in the dermis, and reduce binding of PAH to the glass surface of the receptor chamber (Ellison et al., 2020, 2021). The BSA solution was freshly prepared before each FDC assay.

The receptor chamber is enclosed by a water jacket to regulate the temperature at 32 ± 1 °C corresponding to average skin surface temperature (Lee et al., 2019). The skin was laid atop the upper opening of the FDC so that it covered the receptor chamber. It was fixed by a donor chamber cap and a clamp. The sample solution was added to the donor chamber to start the incubation and the FDCs were occluded with parafilm. After the incubation time, the set-up was disassembled and the compartments were analyzed for their respective analyte concentrations individually: the donor solution was removed and the skin was taken off. The s.c. was stripped off layer by layer with tape strips, which is a common method to determine the concentration profile in the s.c. (Hopf et al., 2020; Simon et al., 2023). The donor solution, the tape strips and the remaining skin were then extracted with acetonitrile. The BSA in the receptor solution was denatured with saturated ethanolic potassium hydroxide, followed by extraction with cyclohexane. Deuterated internal standards were used to compensate for analyte losses throughout sample preparation (SI, section A.2 *Methods*). All resulting solutions were analyzed for their PAH content by gas chromatography coupled to tandem mass spectrometry (GC-MS/MS).

We applied PAH at high concentrations dissolved in squalane (saturated solution for DB[*a,h*]P, 500–1000 µg/ml for other PAH; for exact concentrations, see Table S1) to the skin and incubated for 1 h and 24 h, respectively. For technical reasons, 1 h was the shortest incubation time for which tape stripping could be performed without significant deviations in the incubation times for individual s.c. layers. The 24 h incubation period was chosen because at this time point the system was considered to have approached a steady state.

2.2. Mathematical analysis and calculation

The diffusion of PAH through the s.c. was modelled with an analytical solution to Fick's (1855) second law of diffusion (Eq. (1)). A solution for the one-dimensional diffusion in x-direction through a plane sheet of thickness H_{sc} representing the s.c. is (Herkenne et al., 2007)

$$c_{rel,x,t} = K_{sc/m}\left[1 - \frac{x}{H_{sc}} - \frac{2}{\pi}\sum_{j=1}^{\infty}\frac{1}{j}\sin\left(\frac{j\pi}{H_{sc}}x\right)\exp\left(-\frac{j^2\pi^2 D_{sc}}{H_{sc}^2}t\right)\right], \tag{2}$$

with

$$c_{rel,x,t} = \frac{c_{x,t}}{c_m}, \quad (3)$$

where $c_{x,t}$ is the concentration at a certain depth x at time t in the s.c., c_m is the concentration in the medium applied in the donor chamber, $K_{sc/m}$ is the partition coefficient between the s.c. and the medium, H_{sc} is the thickness of the s.c., j is the index of the infinite series and D_{sc} is the diffusion coefficient in the s.c. The boundary and initial conditions are: (i) c_m is assumed to remain constant over the duration of the incubation period. This is achieved by applying high concentrations close to the solubility limit of the PAH in squalane, that is, quasi-infinite dose conditions. (ii) The s.c. does not contain any analyte at $t = 0$ at any position in x-direction: $c_{x,0} = 0$. This assumption is verified by including negative controls. (iii) The viable epidermis is assumed to act as a perfect sink, with any substance reaching the last layer of the s.c. being removed immediately: $c_{Hsc,t} = 0$.

$K_{sc/m}$ and D_{sc} were obtained by fitting the measured concentration profiles in the s.c. with Eq. (2). The number of terms used in the infinite series was set to 10 000, which was considered sufficiently large to approximate the solution. The data were analyzed using the statistical programming language R (version 4.03), using the non-linear least squares approach.

2.3. Infinite dose conditions

For the determination of $K_{sc/m}$ and D_{sc}, the Organization for Economic Co-operation and Development (OECD) recommends to apply infinite dose conditions in their guidelines on skin penetration studies employing FDC assays (OECD, 2004a, 2004b). This assures that the concentration in the donor solution stays quasi-constant during the course of the experiment. In consequence, steady-state conditions are established at the boundary layer between the medium and the s.c. (Anissimov et al., 2013). We therefore used highly concentrated solutions of PAH in squalane in the present study. Naphthalene, anthracene, pyrene and B[*a*]P were readily dissolved at a concentration of 1 mg·ml^{-1} in squalane after treatment in an ultrasonic bath for 30 min at 70 °C. Due to the lower solubility of DB[*a,h*]P in squalane, a solution of 1 mg·ml^{-1} in dichloromethane was prepared and mixed 1:1 with squalane. Evaporation of dichloromethane under reduced pressure (50 mbar) at 55 °C in a parallel evaporation concentrator (Syncore Analyst, Büchi, Labortechnik AG, Flawil, Switzerland, cooler set to 10 °C) yielded a saturated solution of DB[*a,h*]P. Final PAH concentrations of the applied squalane solutions were determined analytically by GC-MS/MS (Table S1).

2.4. Skin

The skin used in the FDC assays was provided by the Charité , Universitätsmedizin Berlin and treated as described previously (Simon et al., 2023). Briefly, the skin was taken from the flank of female pigs, which had been sacrificed shortly before the skin was removed in an unrelated surgical experiment that did not affect the skin. The excised skin was transported to our laboratory on ice, sheared, cut into pieces of approximately 10 × 20 cm with a knife, and stored at − 20 °C before use. The storage time did not exceed 12 months and skin integrity was thoroughly checked by monitoring the trans-epidermal water loss in line with OECD Guideline 428 (SI, section A.2.3 *Franz diffusion cell protocol*, OECD, 2004b; Zhang et al., 2018).

Pigskin has been used as a substitute for human skin in various previous skin penetration studies (Bartsch et al., 2016, 2018; Gerstel et al., 2016; Herkenne et al., 2006, 2007; Rothe et al., 2017). It was shown that pigskin does not significantly differ from human skin in relevant penetration properties, such as lag time and diffusion of substances in the s.c. (Gerstel et al., 2016; Herkenne et al., 2006; Rothe et al., 2017). For these reasons, the Scientific Committee on Consumer Safety (SCCS) also recommends pigskin to be used in skin penetration studies (SCCS, 2010).

2.5. Thickness of the stratum corneum

The thickness of the porcine s.c. was determined histologically (SI, section A.2.8 *Determination of stratum corneum thickness*). It amounted to 10.14 ± 1.88 µm (mean ± SD, $n = 25$ measurements with three biological replicates, Fig. S2). This is in line with previous studies: Blair (1968) found a thickness of 12.5–17.4 µm for healthy human s.c., Kalia et al. (1996) found a thickness of 9.5–16.1 µm (human s.c.) and Rothe et al. (2017) found 11.1 ± 1.1 µm (human s.c.) and 10.8 ± 2.3 µm (porcine s.c.). During tape stripping, each tape strip removes about one layer of the s.c so that the depth attained is a linear function of the number of tape strips (equation (S6), Simon et al., 2023). The concentrations of PAH in individual s.c. layers as depicted in Figs. 1 and 3 were derived from PAH amounts extracted from individual tape strips and determined via GC-MS/MS. The volume of a single s.c. layer in the FDC assay was calculated assuming an average height of 0.349 µm and a permeation area of 1.76 cm^{-2} of the FDC (see SI, section A.2.3 and equations S5 and S6).

2.6. Concentration of polycyclic aromatic hydrocarbons in the stratum disjunctum

The guidance on dermal absorption of the European Food Safety Authority (EFSA) recommends to dismiss the first tape strip from analysis. The first tape strips removes cells of the *stratum disjunctum* (Buist et al., 2017), the upper most layer of the s.c. which is subject to permanent desquamation. Substances can accumulate in the folds and furrows of the *stratum disjunctum*, which can lead to an over-determination of the concentration in the upper layer of the s.c. In this study, we therefore calculated $K_{sc/m}$ and D_{sc} considering data points from the second tape strip onwards. We expect this to yield more accurate coefficients for a rather homogeneous s.c. The measured concentrations of the first tape strip are represented at negative x-values in the graphs.

3. Results and discussion

3.1. Recovery of PAH in Franz diffusion cell assays

To determine whether quasi-infinite dose conditions were maintained throughout the incubation period, the total PAH recovery across all compartments was calculated (Fig. S3 and Table S1). After 1 h, 97–102% of the applied dose remained in the donor chamber. After 24 h, recovery in the donor compartment ranged between 94% and 97%. These values are in compliance with the OECD guideline that stipulates less than 10% donor depletion to be sufficient for infinite dose conditions (OECD, 2004b).

The viable epidermis and the dermis were found to represent a significant barrier for the higher molecular mass PAH. The concentration of each PAH in the s.c. after 1 h and 24 h exposure was about two to three orders of magnitude higher than the concentration in the remaining skin (see Table 1 for measured PAH concentrations in individual compartments). After 1 h, naphthalene was already detected in the receptor solution whereas only trace amounts of the higher molecular mass PAH were found. After 24 h, the concentration of naphthalene in the receptor solution was more than an order of magnitude higher than the concentration of the other PAH. More lipophilic PAH are thus retained by the rather lipophilic s.c., whereas the comparatively less lipophilic naphthalene is better able to permeate through these compartments. This can be explained by the higher lipophilicity of the s.c. compared to that of the remaining skin, (Gartner, 2021) since PAH are highly lipophilic substances (log$P$ > 3.3, de Lima Ribeiro and Ferreira, 2003; US EPA, 2012).

Interestingly, the concentrations of pyrene and B[*a*]P in the

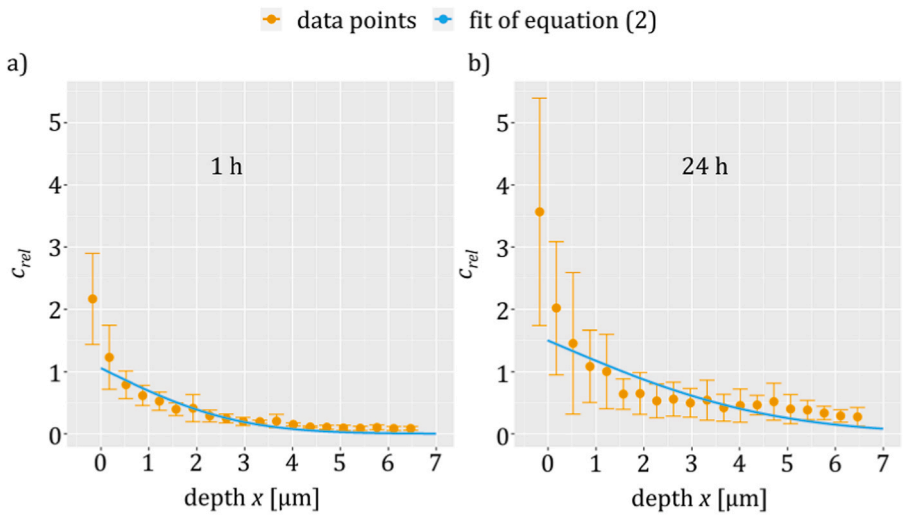

Fig. 1. Measured relative concentrations c_{rel} of B[*a*]P (yellow, mean ± SD) at depth x in the *stratum corneum* and the corresponding fit of the solution of Fick's second law of diffusion (Eq. (2), light blue) after an incubation time of a) 1 h and b) 24 h. The first data points at negative x-values represent the *stratum disjunctum* and were omitted from analysis. For other PAH, see Fig. S4. SD: standard deviation, PAH: polycyclic aromatic hydrocarbons, B[*a*]P: benzo[*a*]pyrene, c_{rel}: see Eq. (3).

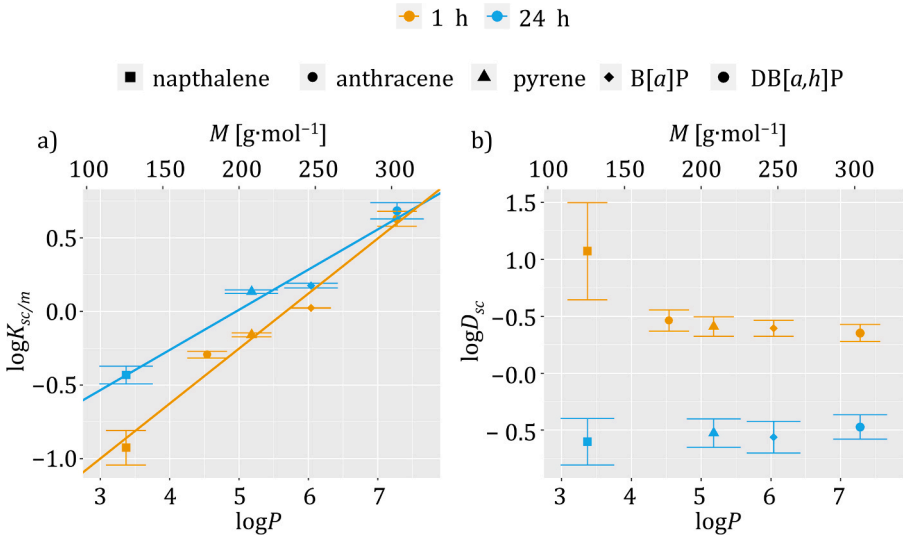

Fig. 2. Calculated a) partition coefficients log$K_{sc/m}$ (mean ± SD) with linear regression curves and b) diffusion coefficients logD_{sc} (mean ± SD) of five PAH for incubation times of 1 h and 24 h (upper x-axis: molecular mass (M), lower x-axis: octanol-water partition coefficient (log$P$). log$P$ and M are linearly related for these PAH (Fig. S5). SD: standard deviation, PAH: polycyclic aromatic hydrocarbons, B[*a*]P: benzo[*a*]pyrene, DB[*a,h*]P: dibenzo[*a,h*]pyrene.

remaining skin after 24 h are significantly higher than that of naphthalene. This might be due to these compounds accumulating at the interface between the s.c. and the viable epidermis. The s.c. of pigskin is not completely removed by 20 tape strips (Simon et al., 2023). Presumably, these compounds are retained in the remaining s.c. layers, diffusing slower into deeper layers of the skin and can thus not reach the receptor in comparable quantities.

3.2. Concentration depth profiles in the stratum corneum

The measured concentrations of PAH in the s.c. decrease with increasing depth (see Fig. 1 for B[*a*]P and Fig. S4 for other investigated PAH). Because the concentration in the donor compartment is quasi-constant (infinite dose conditions), the diffusive loss of PAH in the upper layers of the s.c. will constantly be replenished with PAH from the donor compartment. At the lower end of the s.c. ($x = H_{sc}$), the PAH partition into the viable epidermis. Hence, a constant flux of PAH through the s.c. is maintained in a dynamic equilibrium (steady state), avoiding saturation of s.c. layers.

3.3. Partition coefficients $K_{sc/m}$

The values of $K_{sc/m}$ determined for an incubation time of 1 h are lower than after 24 h (Fig. 2a and Table S2). Partition coefficients describe concentration ratios at chemical equilibrium, which presumably is not yet reached after 1 h. Eq. (2) describes the diffusion through the s.c. at equilibrium between the medium and the most upper s.c. layer. Thus, only when equilibrium is reached, can $K_{sc/m}$ be calculated accurately. After an extended incubation time of 24 h, the system better resembles the steady state. Hence, we consider the values calculated for 24 h as the more realistic partition coefficients $K_{sc/m}$.

Values of log$K_{sc/m}$ for the two different incubation time points linearly depend on log$P$ and the two linear relationships converge for higher log$P$ values (Fig. 2). By extension, log$K_{sc/m}$ is also linearly dependent on the molecular mass M, because log$P$ and M are linearly related for the investigated PAH (Fig. S5, de Lima Ribeiro and Ferreira, 2003; US EPA,

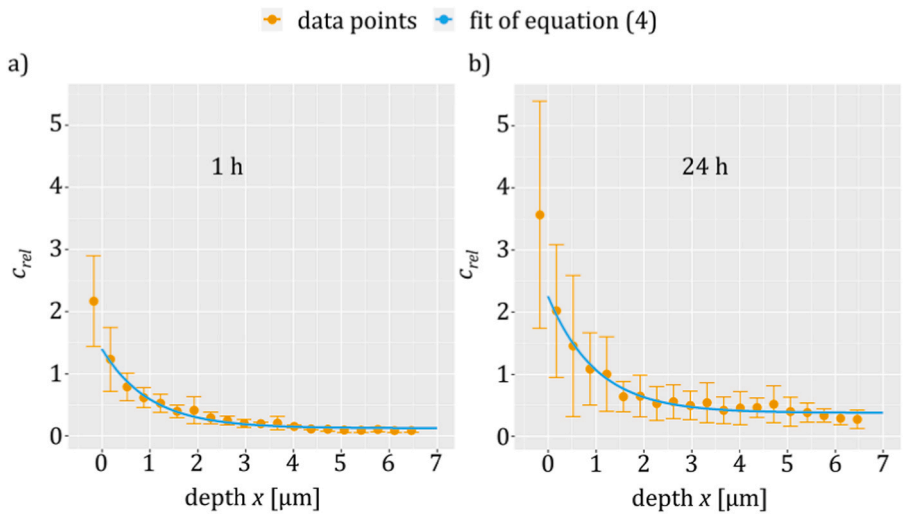

Fig. 3. Alternative fit of an empirically determined function (Eq. (4), light blue) of the relative concentration c_{rel} of B[*a*]P (yellow, mean ± SD) at depth x in the *stratum corneum* after incubation times of a) 1 h and b) 24 h. The first data points at negative x-values represent the *stratum disjunctum* and were omitted from analysis. For other PAH, see Fig. S4. SD: standard deviation, PAH: polycyclic aromatic hydrocarbons, B[*a*]P: benzo[*a*]pyrene, c_{rel}: see Eq. (3).

Table 1
Measured concentrations (mean ± SD) of PAH in different compartments after incubation time t_i. SD: standard deviation, PAH: polycyclic aromatic hydrocarbons, s.c.: *stratum corneum*, B[*a*]P: benzo[*a*]pyrene, DB[*a,h*]P: dibenzo[*a,h*]pyrene, LOQ: limit of quantification; please note the different units of PAH concentrations in individual compartments.

substance	t_i [h]	donor [µg·ml^{-1}]	s.c. [µg·ml^{-1}]	remaining skin [ng·ml^{-1}]	receptor [ng·ml^{-1}]
naphthalene	1	1028 ± 30	63 ± 28	112 ± 24	3.05 ± 0.83
anthracene	1	1027 ± 20	152 ± 55	162 ± 85	0.225 ± 0.304
pyrene	1	532 ± 6	104 ± 31	79 ± 47	0.235 ± 0.245
B[*a*]P	1	644 ± 12	185 ± 53	102 ± 66	0.261 ± 0.331
DB[*a,h*]P	1	51.3 ± 2.7	60 ± 20	74 ± 102	<LOQ
naphthalene	24	916 ± 71	116 ± 100	542 ± 28	425 ± 89
pyrene	24	851 ± 15	679 ± 419	1156 ± 562	19 ± 5
B[*a*]P	24	838 ± 35	499 ± 229	799 ± 364	5 ± 13
DB[*a,h*]P	24	37 ± 25	88 ± 46	181 ± 99	0.86 ± 0.92

2012). DB[*a,h*]P (0.685 ± 0.056) and naphthalene (−0.432 ± 0.060) feature the highest and lowest values for log$K_{sc/m}$, respectively. Notably, the two values derived for DB[*a,h*]P (24 h: 0.685 ± 0.056 vs. 1 h: 0.631 ± 0.052) are not significantly different. This trend indicates that under quasi-infinite dose conditions the more lipophilic PAH also reach steady state faster.

The experimentally determined value for log$K_{sc/m}$ of naphthalene (−0.432 ± 0.060) is considerably lower than reported previously (0.98 ± 0.19, Ellison et al., 2020, 2021) where naphthalene was applied to the skin surface in a 0.88% solution of ethanol in DPBS. Here, we used squalane, which is highly lipophilic (log$P$ = 15.59, Octanol-Water Partition Calculation, 2021). A higher lipophilicity of the medium reduces log$K_{sc/m}$ for lipophilic substances such as PAH. Importantly, squalane represents a medium that is better suited to mimic skin contact to polymer-based consumer products (Barret et al., 2002; Bartsch et al., 2018; Beißmann et al., 2014; Soebianto et al., 1993) and cosmetics, where it is frequently used as an ingredient (Kim and Karadeniz, 2012; Zafar and Chickos, 2019).

3.4. Diffusion coefficients D_{sc}

The calculated values for D_{sc} vary for the two different incubation times (Fig. 2 and Table S2). Eq. (2) requires that the cellular layers beyond the s.c. function as a sink for PAH (boundary condition iii). The flux through the s.c. should thus not be diminished by the solubility of the PAH in the rather hydrophilic viable epidermis. The sink conditions are more likely to be fulfilled at shorter incubation times. Hence, D_{sc} values obtained after 1 h more accurately describe the diffusion process in the s.c. The curvature of the function associated with Eq. (2) is dependent on D_{sc}. With longer incubation times, the contribution of the exponential term (containing D_{sc}) to the measured value of $c_{rel,x,t}$ decreases significantly, leading to a better fit of Eq. (2) at shorter incubation times. Lower residual standard deviations σ of the fit of Eq. (2) describing the concentration profiles measured after 1 h support this conclusion (Table S3).

The presented values for D_{sc} represent the first experimentally determined diffusion coefficients for PAH in the s.c., with the exception of naphthalene. For naphthalene, values between $[2.35 \pm 1.06]\cdot10^{-9}$ m^2·h^{-1} (Ellison et al., 2020, 2021) and $[2.52 \pm 0.84]\cdot10^{-10}$ m^2·h^{-1} (Kim et al., 2008) were reported. These significantly higher coefficients can be attributed to the medium in which naphthalene was applied to the skin. Ellison et al. (2020, 2021) used a 1.12% solution of ethanol in DPBS. Ethanol is known to enhance skin penetration (OECD, 2011). Kim et al. (2006) applied jet fuel as a medium, which has been shown to damage the s.c. (Singh et al., 2003). It is of note that the mentioned studies acknowledge these limitations (Ellison et al., 2020, 2021; Kim et al., 2008). Squalane, on the other hand, is a medium which was shown to not substantially enhance the permeation of applied drugs (Takahashi et al., 1995). D_{sc} for naphthalene ($[1.183 \pm 0.471]\cdot10^{-11}$ m^2·h^{-1}) is higher than for any of the other PAH that were analyzed. Thus, upon dermal exposure, it potentially becomes bioavailable more quickly. However, the lower value for log$K_{sc/m}$ implies lower total amounts of naphthalene in the s.c. compared to the higher molecular mass PAH upon skin contact.

3.5. Simplified mathematical description of diffusion in the stratum corneum

Fick's (1855) laws are the mathematical basis for each discussion of diffusion. As discussed, Eq. (2) represents a solution to Fick's second law. Boundary condition iii states that the viable epidermis must act as a perfect sink. Hence, the concentration at the boundary layer between the s.c. and the viable epidermis (at depth $x = H_{sc} \approx 10$ µm) must always be zero. The viable epidermis, however, is an aqueous matrix and therefore

less lipophilic than the s.c. Thus, after a certain time is passed, a non-zero concentration of PAH in the deepest investigated s.c. layer builds up, even after the shorter incubation period of 1 h (Fig. 1 and Fig. S4). This is supported by the observed underprediction of the concentrations in deeper s.c. layers by the fit of Eq. (2).

We propose a simplified alternative to Eq. (2) to deal with this problem:

$$c_{rel,x,t} = u_t \cdot e^{-x} + w_t, \quad (4)$$

where $c_{rel,x,t}$ is the concentration at depth x and time t divided by the concentration in the donor solution (compare Eq. (3)). The parameters u_t and w_t are time-dependent factors. Eq. (4) describes the data more accurately than Eq. (2) as implied by the lower residual standard deviation σ of the fit (Table S3). It represents an excellent fit to our data for two different time points and for five different substances. We thus hypothesize that Eq. (4) could be used for modelling diffusion through the skin if more data were made available to confirm its suitability for other substance classes.

The parameter w_t can be interpreted as a measure for the retention of a given PAH at the boundary between the s.c. and the viable epidermis. It is time-dependent because the amount of PAH retained at this boundary depends on the amount which is already diffused to this position. We suspect that it is related to the inverse of the removal rate and the viable epidermis/s.c. partition coefficient $K_{ve/sc}$. High removal rates or large coefficients $K_{ve/sc}$, as required for sink conditions, would lead to w_t approaching zero.

logw_t is linearly dependent on log$P$ (Fig. 4b). Since the s.c. is a more lipophilic matrix than the viable epidermis (Gartner, 2021), substances with higher lipophilicity are retained more strongly in the s.c., as observed for the trend of logw_t for different PAH. The parameter logu_t is also linearly correlated with log$P$ (Fig. 4a), as is log$K_{sc/m}$ derived from Eq. (2) (Fig. 2a). Thus, the two parameters are linearly related (Fig. S6).

Eq. (4) does not obey Fick's second law, since that would require w_t to be time-independent (SI, section A2.6 *Mathematical analysis of* Eq. (4)). However, w_t is time-dependent (Fig. 4b). Hence, Eq. (4) describes the diffusion in the s.c. only approximately. Still, this approximation represents an excellent fit to the experimental data. It can be directly correlated to physico-chemical properties, including log$P$ and log$K_{sc/m}$. Additionally, it shows a sound theorized correlation to the removal rate at the s.c./viable epidermis boundary layer and appeals with its simplicity.

4. Conclusion

We demonstrated that the viable epidermis and dermis represent the main barrier for the penetration of higher molecular mass PAH through the skin. Our results indicate that $K_{sc/m}$ can only be calculated reliably from measured concentration profiles of dermally applied substances in the s.c. when a sufficiently long incubation time (for example 24 h) is maintained. Furthermore, for the investigated PAH, log$K_{sc/m}$ is linearly related to log$P$ and M. Values for D_{sc} are highest for naphthalene. For PAH with three or more condensed rings, D_{sc} is lower but comparable to each other. We suspect that naphthalene, due to its low molecular mass and molar volume, features an exceptionally fast diffusion compared to PAH with more extended aromatic ring systems.

We empirically derived a simplified mathematical description of the measured concentration profiles, which fits our data better than the solution to Fick's second law. Its parameters can be correlated to substance- and matrix-specific physico-chemical parameters such as log$P$, $K_{sc/m}$ and the removal rate at the s.c./viable epidermis boundary layer. Future work includes the determination of these constants for other relevant substances in consumer products, such as degradation products of polymer additives.

CRediT authorship contribution statement

Konstantin Simon: Conceptualization, Methodology, Formal analysis, Investigation, Resources, Writing – original draft, Writing – review & editing, Visualization, Project administration. **Lidia Schneider:** Methodology, Formal analysis, Investigation. **Gila Oberender:** Formal analysis, Investigation. **Ralph Pirow:** Methodology, Writing – review & editing. **Christoph Hutzler:** Conceptualization, Methodology, Writing – review & editing. **Andreas Luch:** Writing – review & editing, Resources, Funding acquisition. **Alexander Roloff:** Conceptualization, Methodology, Formal analysis, Resources, Writing – original draft, Writing – review & editing, Supervision, Project administration, Funding acquisition.

Declaration of Competing Interest

The authors declare that they have no known competing financial interests or personal relationships that could have appeared to influence the work reported in this paper.

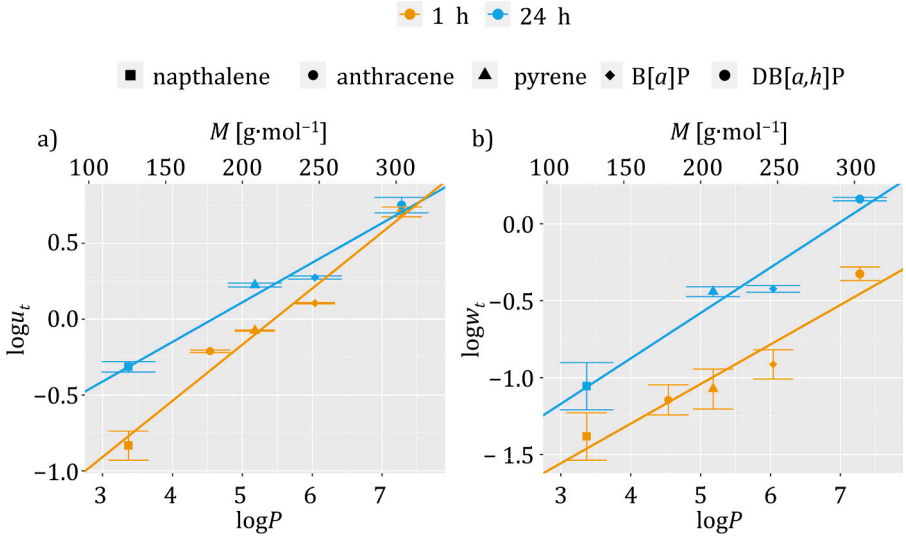

Fig. 4. a) logu_t (mean ± SD) vs. octanol-water partition coefficient (log$P$) with linear regression curves and b) logw_t (mean ± SD) vs. log$P$ of five PAH for incubation times of 1 h and 24 h (upper x-axis: molecular mass (M), lower x-axis: log$P$. log$P$ and M are linearly related for these PAH (Fig. S5). SD: standard deviation, PAH: polycyclic aromatic hydrocarbons, B[a]P: benzo[a]pyrene, DB[a,h]P: dibenzo[a,h]pyrene.

Data availability

Data will be made available on request.

Acknowledgements

We thank Tanja Schmidt and Katja Reiter from Charité for providing us with pigskin. We thank Klaudia Michna and Svetlana Kruschinski for excellent technical assistance. We thank Franziska Riedel, Benjamin-Christoph Krause, Charlotte Kromer, Aline Rosin and Nadja Mallock for proof reading and fruitful discussions. This work was funded by BfR-internal grants BfR-CPS-08-1322–514 and BfR-CPS-08-1322–774.

Appendix A. Supporting information

Supplementary data associated with this article can be found in the online version at doi:10.1016/j.ecoenv.2023.115113.

References

Alawi, M.A., Abdullah, R.A., Tarawneh, I., 2018. Determination of polycyclic aromatic hydrocarbons (PAHs) in carbon black-containing plastic consumer products from the Jordanian market. Toxin Rev. 37 (4), 269–277. https://doi.org/10.1080/15569543.2017.1359628.

Anissimov, Y.G., Jepps, O.G., Dancik, Y., Roberts, M.S., 2013. Mathematical and pharmacokinetic modelling of epidermal and dermal transport processes. Adv. Drug Del. Rev. 65 (2), 169–190. https://doi.org/10.1016/j.addr.2012.04.009.

Barret, J., Gijsman, P., Swagten, J., Lange, R.F., 2002. A molecular study towards the interaction of phenolic anti-oxidants, aromatic amines and HALS stabilizers in a thermo-oxidative ageing process. Polym. Degrad. Stab. 76 (3), 441–448. https://doi.org/10.1016/S0141-3910(02)00047-2.

Bartsch, N. Polymer additives, contaminants and non-intentionally added substances in consumer products: Combined migration, permeation and toxicity analyses in skin. Doctoral dissertation, Freie Universität, Berlin, 2018.

Bartsch, N., Hutzler, C., Vieth, B., Luch, A., 2017. Target analysis of polycyclic aromatic hydrocarbons (PAHs) in consumer products and total content of polycyclic aromatic compounds (PACs). Polycycl. Aromat. Compd. 37 (2–3), 114–121. https://doi.org/10.1080/10406638.2016.1189440.

Bartsch, N., Heidler, J., Vieth, B., Hutzler, C., Luch, A., 2016. Skin permeation of polycyclic aromatic hydrocarbons: a solvent-based in vitro approach to assess dermal exposures against benzo[a]pyrene and dibenzopyrenes. J. Occup. Environ. Hyg. 13 (12), 969–979. https://doi.org/10.1080/15459624.2016.1200724.

Bartsch, N., Girard, M., Schneider, L., Weijgert, V.V.D., Wilde, A., Kappenstein, O., Vieth, B., Hutzler, C., Luch, A., 2018. Chemical stabilization of polymers: Implications for dermal exposure to additives. J. Environ. Sci. Heal. A 53 (5), 405–420. https://doi.org/10.1080/10934529.2017.1412192.

Beißmann, S., Reisinger, M., Grabmayer, K., Wallner, G., Nitsche, D., Buchberger, W., 2014. Analytical evaluation of the performance of stabilization systems for polyolefinic materials. Part I: Interactions between hindered amine light stabilizers and phenolic antioxidants. Polym. Degrad. Stab. 110, 498–508. https://doi.org/10.1016/j.polymdegradstab.2014.09.020.

Wilma F. Bergfeld, D. V. B, Ronald A. Hill, Curtis D. Klaassen, Daniel C. Liebler, James G. Marks, Jr., Ronald C. Shank, Thomas J. Slaga, and Paul W. Snyder In Safety Assessment of Squalane and Squalene *as Used in Cosmetics*, 2019.

Blair, C., 1968. Morphology and thickness of the human stratum corneum. Br. J. Dermatol. 80 (7), 430–436. https://doi.org/10.1111/j.1365-2133.1968.tb11978.x.

Brinkmann, J., Stolpmann, K., Trappe, S., Otter, T., Genkinger, D., Bock, U., Liebsch, M., Henkler, F., Hutzler, C., Luch, A., 2012. Metabolically competent human skin models: activation and genotoxicity of benzo[a]pyrene. Toxicol. Sci. 131 (2), 351–359. https://doi.org/10.1093/toxsci/kfs316.

Bronaugh, R.L., Stewart, R.F., 1984. Methods for in vitro percutaneous absorption studies III: hydrophobic compounds. J. Pharm. Sci. 73 (9), 1255–1258. https://doi.org/10.1002/jps.2600730916.

Bronaugh, R.L., Stewart, R.F., 1986. Methods for in vitro percutaneous absorption studies VI: preparation of the barrier layer. J. Pharm. Sci. 75 (5), 487–491. https://doi.org/10.1002/jps.2600750513.

Bronaugh, R.L., Congdon, E.R., Scheuplein, R.J., 1981. The effect of cosmetic vehicles on the penetration of N-nitrosodiethanolamine through excised human skin. J. Invest. Dermatol. 76 (2), 94–96. https://doi.org/10.1111/1523-1747.ep12525384.

Comission Regulation (EU) No 1272/2013 amending Annex XVII to Regulation (EC) No 1907/2006 (REACH). Official Journal of the European Union 328, 2013, 69–71.

Bronaugh, R.L., Stewart, R.F., Simon, M., 1986. Methods for in vitro percutaneous absorption studies VII: use of excised human skin. J. Pharm. Sci. 75 (11), 1094–1097. https://doi.org/10.1002/jps.2600751115.

Buist, H.; Craig, P.; Dewhurst, I.; Hougaard Bennekou, S.; Kneuer, C.; Machera, K.; Pieper, C.; Court Marques, D.; Guillot, G., Guidance on dermal absorption. In EFSA Journal, European Food Safety Authority, Ed. 2017; Vol. 15, p e04873.

Bundesinstitut für Risikobewertung (BfR): PAH levels in consumer products should be as low as possible. 2019 ⟨https://www.bfr.bund.de/en/press_information/2019/29/pah_levels_in_consumer_products_should_be_as_low_as_possible-241757.html⟩ (accessed 26.08.2021).

Collins, J., Brown, J., Alexeeff, G., Salmon, A., 1998. Potency equivalency factors for some polycyclic aromatic hydrocarbons and polycyclic aromatic hydrocarbon derivatives. Regul. Toxicol. Pharmacol. 28 (1), 45–54. https://doi.org/10.1006/rtph.1998.1235.

Ellison, C.A., Tankersley, K.O., Obringer, C.M., Carr, G.J., Manwaring, J., Rothe, H., Duplan, H., Géniès, C., Grégoire, S., Hewitt, N.J., 2020. Partition coefficient and diffusion coefficient determinations of 50 compounds in human intact skin, isolated skin layers and isolated stratum corneum lipids. Toxicol. Vitr. 69, 104990 https://doi.org/10.1016/j.tiv.2020.104990.

Ellison, C.A., Tankersley, K.O., Obringer, C.M., Carr, G.J., Manwaring, J., Rothe, H., Duplan, H., Géniès, C., Grégoire, S., Hewitt, N.J., 2021. Corrigendum to partition coefficient and diffusion coefficient determinations of 50 compounds in human intact skin, isolated skin layers and isolated stratum corneum lipids. Toxicol. Vitr. 71, 105050 https://doi.org/10.1016/j.tiv.2020.105050.

Fick, A., 1855. Ueber diffusion. Ann. Phys. (Leipz.) 170 (1), 59–86.

Franz, T.J., 1975. Percutaneous absorption. On the relevance of in vitro data. J. Invest. Dermatol. 64 (3), 190–195. https://doi.org/10.1111/1523-1747.ep12533356.

Gartner, L.P., 2021. Integument. *Textbook of Histology*, 5 ed..,. Elsevier,.

International Agency for Research on Cancer (IARC), 2010. Some non-heterocyclic polycyclic aromatic hydrocarbons and some related exposures. IARC Monogr. Eval. Carcinog. Risks Hum. 92, 1.

Gerstel, D., Jacques-Jamin, C., Schepky, A., Cubberley, R., Eilstein, J., Grégoire, S., Hewitt, N., Klaric, M., Rothe, H., Duplan, H., 2016. Comparison of protocols for measuring cosmetic ingredient distribution in human and pig skin. Toxicol. Vitr. 34, 153–160. https://doi.org/10.1016/j.tiv.2016.03.012.

Hardin, J.A., Hinoshita, F., Sherr, D.H., 1992. Mechanisms by which benzo[a]pyrene, an environmental carcinogen, suppresses B cell lymphopoiesis. Toxicol. Appl. Pharmacol. 117 (2), 155–164. https://doi.org/10.1016/0041-008X(92)90232-H.

Herkenne, C., Naik, A., Kalia, Y.N., Hadgraft, J., Guy, R.H., 2006. Pig ear skin ex vivo as a model for in vivo dermatopharmacokinetic studies in man. Pharm. Res. 23 (8), 1850–1856. https://doi.org/10.1007/s11095-006-9011-8.

Herkenne, C., Naik, A., Kalia, Y.N., Hadgraft, J., Guy, R.H., 2007. Ibuprofen transport into and through skin from topical formulations: in vitro–in vivo comparison. J. Invest. Dermatol. 127 (1), 135–142. https://doi.org/10.1038/sj.jid.5700491.

Hopf, N., Champmartin, C., Schenk, L., Berthet, A., Chedik, L., Du Plessis, J., Franken, A., Frasch, F., Gaskin, S., Johanson, G., 2020. Reflections on the OECD guidelines for in vitro skin absorption studies. Regul. Toxicol. Pharmacol., 104752 https://doi.org/10.1016/j.yrtph.2020.104752.

International Agency for Research on Cancer (IARC), 2018, Agents classified by the IARC monographs, volumes 1–113. https://monographs.iarc.who.int/agents-classified-by-the-iarc/ (accessed 13.08.2021).

Kalia, Y.N., Pirot, F., Guy, R.H., 1996. Homogeneous transport in a heterogeneous membrane: water diffusion across human stratum corneum in vivo. Biophys. J. 71 (5), 2692–2700. https://doi.org/10.1016/S0006-3495(96)79460-2.

Kim, D., Andersen, M.E., Nylander-French, L.A., 2006. Dermal absorption and penetration of jet fuel components in humans. Toxicol. Lett. 165 (1), 11–21. https://doi.org/10.1016/j.toxlet.2006.01.009.

Kim, D., Farthing, M.W., Miller, C.T., Nylander-French, L.A., 2008. Mathematical description of the uptake of hydrocarbons in jet fuel into the stratum corneum of human volunteers. Toxicol. Lett. 178 (3), 146–151. https://doi.org/10.1016/j.toxlet.2008.03.005.

Kim, S.-K., Karadeniz, F., 2012. Biological importance and applications of squalene and squalane. Adv. Food Nutr. Res 65, 223–233. https://doi.org/10.1016/B978-0-12-416003-3.00014-7.

Lee, C.M., Jin, S.P., Doh, E.J., Lee, D.H., Chung, J.H., 2019. Regional Variation of Human Skin Surface Temperature. Ann. Dermatol. 31 (3), 349–352. https://doi.org/10.5021/ad.2019.31.3.349.

de Lima Ribeiro, F.A., Ferreira, M.M.C., 2003. QSPR models of boiling point, octanol–water partition coefficient and retention time index of polycyclic aromatic hydrocarbons. J. Mol. Struc. -THEOCHEM 663 (1–3), 109–126. https://doi.org/10.1016/j.theochem.2003.08.107.

Luo, K., Zeng, D., Kang, Y., Lin, X., Sun, N., Li, C., Zhu, M., Chen, Z., Man, Y.B., Li, H., 2020. Dermal bioaccessibility and absorption of polycyclic aromatic hydrocarbons (PAHs) in indoor dust and its implication in risk assessment. Environ. Pollut. 264, 114829 https://doi.org/10.1016/j.envpol.2020.114829.

Mackenzie, K.M., Murray Angevine, D., 1981. Infertility in mice exposed in utero to benzo[a]pyrene. Biol. Reprod. 24 (1), 183–191. https://doi.org/10.1095/biolreprod24.1.183.

Moody, R.P., Nadeau, B., Chu, I., 1995. In vivo and in vitro dermal absorption of benzo [a]pyrene in rat, guinea pig, human and tissue-cultured skin. J. Dermatol. Sci. 9 (1), 48–58. https://doi.org/10.1016/0923-1811(94)00356-J.

Moody, R.P., Tytchino, A.V., Yip, A., Petrovic, S., Novel, A., 2011. "By Difference" Method for Assessing Dermal Absorption of Polycyclic Aromatic Hydrocarbons from Soil at Federal Contaminated Sites. J. Toxicol. Environ. Health, A 74 (19), 1294–1303. https://doi.org/10.1080/15287394.2011.589104.

Ng, K.M.E., Bronaugh, R.L., Franklin, C.A., Somers, D.A., 1991. Percutaneous absorption/metabolism of phenanthrene in the hairless guinea pig: Comparison of in vitro and in vivo results. Fundam. Appl. Toxicol. 16 (3), 517–524. https://doi.org/10.1016/0272-0590(91)90092-I.

Ng, S.-F., Rouse, J.J., Sanderson, F.D., Meidan, V., Eccleston, G.M., 2010. Validation of a static Franz diffusion cell system for in vitro permeation studies. AAPS PharmSciTech 11 (3), 1432–1441. https://doi.org/10.1208/s12249-010-9522-9.

Octanol-Water Partition Calculation. ⟨http://www.chemspider.com/Chemical-Structure.7798.html?rid=a22a50c7–1c8c-446d-949a-5abd6fe95e4e⟩ (accessed 20.09.2021).

OECD Series on Testing and Assesment No. 28: Guidance document for the conduct of skin absorption studies. OECD Publishing: Paris, 2004a.
OECD Guideline for the Testing of Chemicals No. 428: Skin Absorption: in vitro Method. OECD Publishing: Paris, 2004b.
OECD Environment Directorate: Health and Safety Publications Series on Testing and Assessment No. 156: Guidance Notes on Dermal Absorbtion. OECD Publishing: Paris, 2011.
Raykar, P.V., Fung, M.C., Anderson, B.D., 1988. The role of protein and lipid domains in the uptake of solutes by human stratum corneum. Pharm. Res 5 (3), 140–150. https://doi.org/10.1023/a:1015956705293.
Regulation (EC) Nr. 1907/2006 (REACH). In Official Journal of the European Union, 2006; Vol. 136, pp 3–280.
Rota, M., Bosetti, C., Boccia, S., Boffetta, P., La Vecchia, C., 2014. Occupational exposures to polycyclic aromatic hydrocarbons and respiratory and urinary tract cancers: an updated systematic review and a meta-analysis to 2014. Arch. Toxicol. 88 (8), 1479–1490. https://doi.org/10.1007/s00204-014-1296-5.
Rothe, H., Obringer, C., Manwaring, J., Avci, C., Wargniez, W., Eilstein, J., Hewitt, N., Cubberley, R., Duplan, H., Lange, D., 2017. Comparison of protocols measuring diffusion and partition coefficients in the stratum corneum. J. Appl. Toxicol. 37 (7), 806–816. https://doi.org/10.1002/jat.3427.
Roy, T.A., Kriech, A.J., Mackerer, C.R., 2007. Percutaneous absorption of polycyclic aromatic compounds from bitumen fume condensate. J. Occup. Environ. Hyg. 4 (sup1), 137–143. https://doi.org/10.1080/15459620701334814.
Sartorelli, P., Aprea, C., Cenni, A., Novelli, M.T., Orsi, D., Palmi, S., Matteucci, G., 1998. Prediction of percutaneous absorption from physicochemical data: a model based on data of in vitro experiments. Ann. Occup. Hyg. 42 (4), 267–276. https://doi.org/10.1016/S0003-4878(98)00021-0.
SCCS (Scientific Committee on Consumer Safety): Basic criteria for the in vitro assessment of dermal absorption of cosmetic ingredients. 7th plenary meeting 2010.
Simon, K., Oberender, G., Roloff, A., 2023. Continuous removal of single cell layers by tape stripping the stratum corneum – a histological study. Eur. J. Pharm. Biopharm. 188, 48–53. https://doi.org/10.1016/j.ejpb.2023.04.022.
Singh, S., Zhao, K., Singh, J., 2003. In vivo percutaneous absorption, skin barrier perturbation, and irritation from JP-8 jet fuel components. Drug Chem. Toxicol. 26 (2), 135–146. https://doi.org/10.1081/DCT-120020408.
Soebianto, Y.S., Katsumura, Y., Ishigure, K., Kubo, J., Koizumi, T., Shigekuni, H., Azami, K., 1993. Model experiment on the protection effect in polymers: radiolysis of liquid squalane in the presence and absence of additives. Polym. Degrad. Stab. 42 (1), 29–40. https://doi.org/10.1016/0141-3910(93)90022-B.
Sousa, G., Teixeira, J., Delerue-Matos, C., Sarmento, B., Morais, S., Wang, X., Rodrigues, F., Oliveira, M., 2022. Exposure to PAHs during Firefighting Activities: A Review on Skin Levels, In Vitro/In Vivo Bioavailability, and Health Risks. Int. J. Environ. Res. Public Health 19 (19). https://doi.org/10.3390/ijerph191912677.
Takahashi, K., Suzuki, T., Sakano, H., Mizuno, N., 1995. Effect of vehicles on diclofenac permeation across excised rat skin. Biol. Pharm. Bull. 18 (4), 571–575. https://doi.org/10.1248/bpb.18.571.
US EPA. Estimation Program Interface (EPI) Suite. Ver. 4.11. 2012, Available from, as of Sept 13, 2016: ⟨https://www2012.epa.gov/tsca-screening-tools⟩.
Zafar, A., Chickos, J., 2019. The vapor pressure and vaporization enthalpy of squalene and squalane by correlation gas chromatography. J. Chem. Thermodyn. 135, 192–197. https://doi.org/10.1016/j.jct.2019.03.032.
Zhang, Q., Murawsky, M., LaCount, T., Kasting, G.B., Li, S.K., 2018. Transepidermal water loss and skin conductance as barrier integrity tests. Toxicol. Vitr. 51, 129–135. https://doi.org/10.1016/j.tiv.2018.04.009.